

A DEMONSTRATION APPARATUS FOR POROELASTIC MECHANICS

THOMAS M. QUINN

McGill University • Montreal, QC, Canada

The mechanics of poroelastic materials were first elucidated by Biot for purposes of describing consolidation and acoustic properties of saturated soils and porous rock.^[1] This seminal work has since been adapted for specific purposes in describing the mechanics and electromechanics of gels^[2, 3] and biological tissues.^[4, 5] An understanding of poroelastic mechanics therefore underlies advanced undergraduate- and graduate-level study in a diverse range of fields including oil recovery,^[6] geomechanics,^[7] manufacturing of composite materials,^[8] myriad applications of gels,^[9, 10] and soft tissue biophysics.^[11, 12]

From a teaching perspective, a theoretical description of poroelastic mechanics is typically most easily introduced together with the idealized phenomena of one-dimensional creep and stress relaxation.^[5, 13] Creep refers to a change in material thickness (or length) under constant applied force while stress relaxation refers to a change in measured stress under constant thickness. In both cases, macroscopic thickness and confining force (stress) are related to strain, pressure, and fluid velocity fields at the microscale. These phenomena provide a starting point for presentation of a poroelastic mechanical description because practical examples (*e.g.*, soil consolidation under new buildings^[14]; diurnal variations in human height due to intervertebral disk consolidation^[15]) motivate the need for quantitative study, and their well-defined physical nature makes them suitable first examples of application of the theory. Therefore a clear visualization of creep and stress relaxation in terms of their macroscopic appearance and the associated underlying changes in microstructure is advantageous to students at an early stage of exposure to the subject.

Typically, attempts to help students visualize creep and stress relaxation are made using professor-drawn sketches or computer simulations. Strain fields internal to the poroelastic medium and boundary conditions relating to fluid flows and pressures at boundaries are presented abstractly, and students must assimilate this information without the benefit of observation of the actual phenomena. In contrast, a physical demonstration functions “by itself” and without the direct influence of the professor; the physical phenomena under consideration are in plain view. Interactive lecture demonstrations (ILDs) have been shown to provide substantial and significant learning gains at the early undergraduate physics level,^[16, 17] and it is reasonable to expect that demonstrations may achieve similar results at more advanced stages of learning. Furthermore, a physical model provides students with an immediate opportunity to experiment and obtain feedback for their developing intuition for poroelastic mechanics once the theory has been presented and applied to relatively simple examples. Therefore, we developed a classroom demonstra-

Thomas M. Quinn received a B.Sc. in engineering physics from Queen's University and a Ph.D. in mechanical and medical engineering from the Harvard-MIT Division of Health Sciences and Technology. After post-doctoral fellowships at the University of Bern and the Ecole Polytechnique Federale de Lausanne, he returned to his native Canada where he became an associate professor in the Department of Chemical Engineering at McGill University.



© Copyright ChE Division of ASEE 2013

tion that is straightforward to assemble, can be easily modified to alter material properties and time scales for creep and stress relaxation, and provides several possibilities for development of students' abilities to visualize poroelastic mechanical phenomena. It can also be used to illustrate convective dispersion of small solutes in dynamically compressed poroelastic media, which is a rich "follow-on" topic for study once a solid understanding of poroelastic mechanics has been achieved.

APPARATUS DESCRIPTION

The demonstration apparatus consists of a hollow acrylic (transparent Plexiglas) column mounted vertically, filled with water and a series of cylindrical polystyrene blocks separated by springs (Figure 1). When immersed in water, the polystyrene blocks are nearly neutrally buoyant (density 1.05 g/cm^3) so that separation between the blocks is maintained without significant spring compression. Spring stiffness determines the elastic modulus for one-dimensional compression along the column axis. Movement of the polystyrene blocks relative to the acrylic column requires fluid flow between a thin annular space between the blocks and the column; this determines the hydraulic permeability of the structure. Details given in the Appendix provide specific geometries and properties for these components that have been implemented successfully in our department.

PRESENTATION AND DATA ANALYSIS

Creep and stress relaxation during a single load-release cycle—starting from the free-swelling state, the apparatus can be used to illustrate compressive creep and then stress relaxation to a compressed mechanical equilibrium, followed by expansive creep to re-attain the free-swelling equilibrium state. For the apparatus described, this full sequence takes approximately 1-2 minutes, so there is ample opportunity to repeat it several times in a single lecture in order to focus on different aspects of the consolidation process with each repeat demonstration. In the free-swelling state, uniform zero strain is evident throughout the column from the regular distribution of blocks and intervening spaces (Figure 2a). Compressive creep is initiated by inserting the handle of the hammer into the top of the column until it contacts the uppermost polystyrene block and then releasing it (Figure 2b). The column thickness subsequently decreases under the near-constant weight of the hammer until the head of the hammer is blocked from entering the column; this creep transition lasts approximately 10 seconds (Figure 2c-f). (The hammer weight is offset slightly by the buoyant effect of the water displaced by the handle as it descends, therefore the force applied is not perfectly constant.) During this period it is helpful to emphasize the dramatic increase in compressive strain taking place at the top of the column, contrasted with negligible changes in strain at

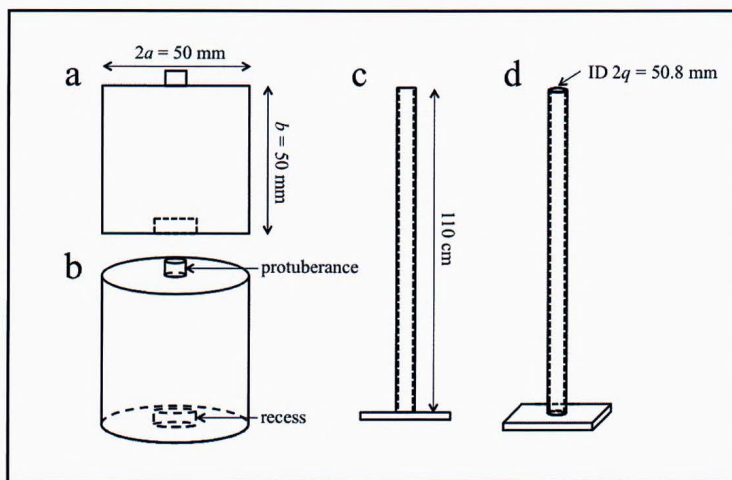


Figure 1. a) Drafting sketch of a polystyrene block. Blocks were cylinders of 50 mm length \times 50 mm diameter, with a protuberance and recess on opposite axial faces for mounting of conical compression springs. b) 3-D sketch of a polystyrene block. c) Drafting sketch of the acrylic column. The column was transparent with an inner diameter of 50.8 mm, and mounted vertically on an acrylic base. d) 3-D sketch of the column.

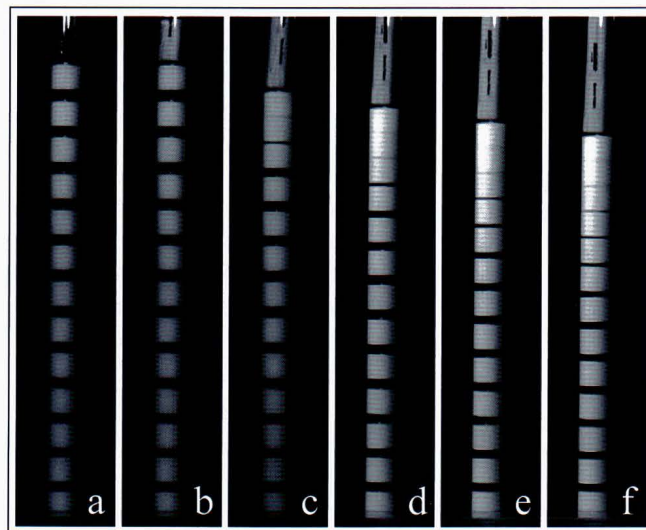


Figure 2. Demonstration of the early stages of compressive creep. a) The demonstration apparatus in its free-swelling state. b) To initiate creep, the handle of a 4 lb. sledgehammer is brought into contact with the uppermost polystyrene block and then released onto the column at time $t=0$. Increasing consolidation in the upper region of the column is evident at c) $t=2$, d) $t=4$, e) $t=6$, and f) $t=8$ seconds.

the bottom. Column thickness reductions can only occur with expulsion of water, so this is also an opportunity to emphasize that fluid flows vertically upward, and that the pressure field in the column must have been altered by the presence of the hammer such that pressure increases with depth (over and above the "background" hydrostatic pressure field). When

the head of the hammer comes to rest atop the acrylic tube (Figure 3a), the column is subsequently held at constant thickness and a stress relaxation transient begins (Figure 3b). At this point it is useful to emphasize that stress relaxation involves (mathematically speaking) “diffusive transport” of strain from high concentrations near the top of the column to relatively low concentrations at the bottom. A redistribution of fluid and solid occurs such that strain, or solid content, is transported downward while fluid is transported upward (Figure 3c-f). At the end of stress relaxation, a compressed mechanical equilibrium is established where strain is again distributed uniformly throughout the column (Figure 4a). Removal of the hammer from the column initiates another creep transient (Figure 4b), this time expansive in nature and under a constant zero load. In contrast to compressive creep, this time the upper regions of the column are relatively high in water content relative to the deeper regions (Figure 4c) as fluid is transported downward and the blocks in the column move upward to re-attain the free-swelling thickness (Figure 4d-f). It is interesting to note that the characteristic time over which stress relaxation occurs (approximately 10 seconds for the apparatus described) is significantly smaller than for the expansive creep transient (approximately 100 seconds). These

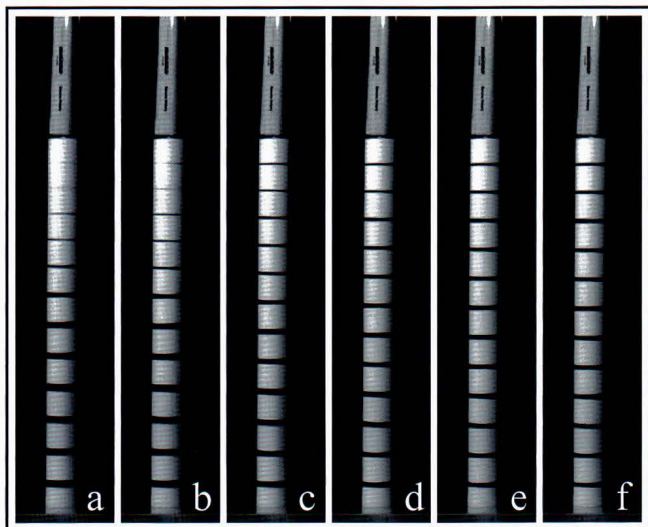


Figure 3. Demonstration of stress relaxation. Compressive creep under the weight of a 4 lb. sledgehammer terminates when the head of the hammer abuts atop the acrylic tube, stopping the hammer’s downward motion and defining time $t=0$ for the ensuing stress relaxation transient. a) Just before time $t=0$ and b) $t=0$, from which point the column thickness is constant. The initial condition for stress relaxation involves large compressive strains (extensive dehydration) in the upper region of the column and relatively small strains in the lower region. Diffusion of strain and the redistribution of fluid and solid within the column to attain a new mechanical equilibrium under uniform strain are evident at c) $t=2$, d) $t=4$, e) $t=6$, and f) $t=8$ seconds.

rough quantifications are useful for comparison to theoretical models for creep and stress relaxation to be made subsequently (below) and for evaluation of the accuracy of models of the poroelastic properties of the demonstration apparatus.

Poroelastic mechanics: a “diffusion” governing equation for strain – For one-dimensional consolidation (in the x -direction), the mechanics of poroelastic materials may be summarized by four basic equations. Darcy’s Law relates fluid velocity (volume flux) U to gradients in pressure p

$$U_x = -\frac{k}{\mu} \frac{dp}{dx} \quad (1)$$

where k is hydraulic permeability and μ is fluid viscosity. Application of Newton’s second law to a deforming poroelastic material under the condition that inertia is negligible provides

$$\frac{d}{dx}(p + \sigma) = 0 \quad (2)$$

where σ is the stress arising from deformation of the solid component of the material. Assuming linear elasticity implies

$$H_A = \frac{\Delta\sigma}{\Delta\varepsilon} \quad (3)$$

where H_A is the “bulk longitudinal” or “confined compression” modulus of elasticity and ε is compressive strain. Fluid

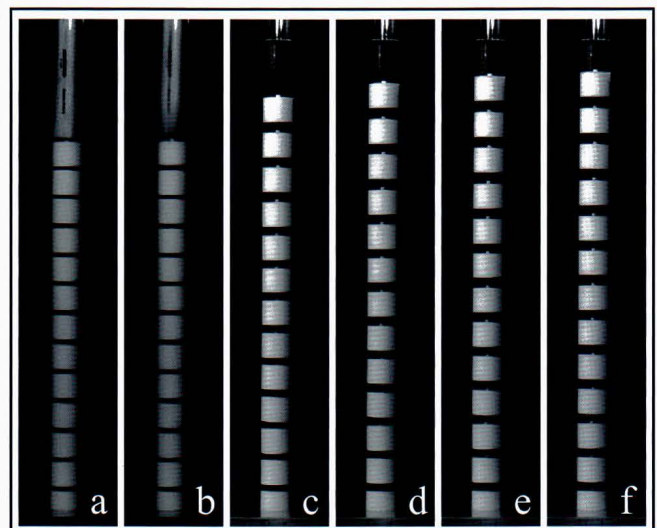


Figure 4. Demonstration of expansive creep to a free-swelling equilibrium. a) The demonstration apparatus in a compressed state, after stress relaxation has proceeded to mechanical equilibrium. b) To initiate expansive creep, the 4 lb. sledgehammer is removed from the column at time $t=0$, from which point zero external force is applied to the uppermost polystyrene block. Column thickness subsequently increases until free-swelling equilibrium is attained. Swelling (decreased compressive strain) is evident primarily in the upper region of the column at early stages of expansive creep at c) $t=20$ seconds, then throughout the column at d) $t=40$, e) $t=60$, and f) $t=80$ seconds.

continuity provides

$$\frac{dU_x}{dx} = \frac{\dot{\epsilon}}{1-\epsilon} \quad (4)$$

Combination of Eqs. (1)-(4) shows that for small departures from an equilibrium strain ϵ_e the compressive strain is governed by a diffusion equation

$$\dot{\epsilon} \equiv \frac{d\epsilon}{dt} = D_M \frac{d^2\epsilon}{dx^2} \quad (5)$$

where the mechanical diffusivity D_M is determined by material properties at ϵ_e :

$$D_M = \frac{H_A \epsilon_e k_c}{\mu} (1 - \epsilon_e) \quad (6)$$

For many poroelastic materials, H_A and k are functions of strain [Eq. (6)]; closer analysis of how these properties depend upon the structure of the demonstration apparatus provides insight into how these strain-dependencies arise.

Thickness and strain – In the demonstration apparatus, overall thickness is the distance from the bottom of the column to the top of the uppermost polystyrene block. This includes 12 springs separating 13 blocks (Figures 2-4), resulting in a thickness of approximately 91 cm in the free-swelling state (Figure 2a). Ignoring the one extra block, the column is essentially constructed of 12 repeating units where 1 unit is a block and spring. If b represents block length and h_i is the space between adjacent blocks associated with the i th repeating unit, then the local compressive strain (decrease in thickness normalized to free-swelling thickness) within the column is given by

$$\epsilon_i = \frac{h_0 - h_i}{b + h_0} \quad (7)$$

where h_0 is the space between blocks in the free-swelling state. Therefore compressive strain is linearly related to h_i in the apparatus. At mechanical equilibrium, the apparatus exhibits nearly uniform h throughout the column (perfect uniformity is, however, not achieved since the polystyrene blocks are not exactly neutrally buoyant), reflecting uniform strain.

Hydraulic permeability – Hydraulic permeability may be estimated by considering flows in the annular space between polystyrene blocks and the acrylic tube, in series with zones of very high permeability in the space between polystyrene blocks. For fully developed, zero Reynolds number flows in the annular space around the blocks, the relationship between area-averaged (over the tube cross-section) flow and pressure gradient provides a “block permeability” k_b

$$k_b = \frac{q^4 - a^4}{8q^2} - \frac{(q^2 - a^2)^2}{8q^2 \ln \frac{q}{a}} \quad (8)$$

where a is the outer radius of the blocks and q is the inner ra-

dius of the tube. This creeping flow calculation is reminiscent of permeability estimation in other porous media^[18]; however, an estimation of the Reynolds number for the apparatus described indicates that it is of order 1, and therefore Eq. (8) can only be considered a rough estimate. Nevertheless, assuming that the pressure-flow relation for the space between blocks results in a permeability which is much larger than k_b , and that for each repeating unit the permeabilities for the block and the space between blocks may be treated like conductances in series, one obtains

$$k_i = k_b \frac{(b + h_i)}{b} \quad (9)$$

This result, while approximate, nevertheless emphasizes that the local permeability within the column (k_i) depends upon h_i , or the local strain [Eq. (7)].

Elastic modulus – The confined compression modulus in the demonstration apparatus is given by the stress vs. strain relation. Assuming a linear force-displacement relation for the springs represented by the spring constant k_s , the stress associated with a change of the space between blocks from h_0 to h_i is given by

$$\sigma_i = k_s \frac{(h_0 - h_i)}{A} \quad (10)$$

where A is the cross-sectional area inside the tube ($A = \pi q^2$). Combining this with Eq. (7) provides

$$H_A = k_s \frac{b + h_0}{A} \quad (11)$$

Boundary conditions and characteristic times – The demonstration apparatus represents a poroelastic continuum undergoing one-dimensional confined compression, with an impermeable surface at the bottom and a permeable surface at the top. Since fluid flow at the bottom is impossible, com-

bination of Eqs. (1), (2), and (3) shows that $\frac{d\epsilon}{dx} = 0$ always applies at that boundary. During creep transitions, constant stresses applied at the top of the column (where the fluid is constrained to be near atmospheric pressure) imply that strain is constant there. Solution of Eq. (5) for these conditions^[5, 13] shows that the kinetics of creep transients are dominated by a decaying exponential with time constant

$$\tau_{\text{creep}} = \frac{4d^2}{\pi^2 D_M} \quad (12)$$

where d represents total column thickness. During stress relaxation, column thickness is held constant which implies

no fluid flow and $\frac{d\epsilon}{dx} = 0$ at both boundaries. Solution of Eq. (5)^[5, 13] then shows that the kinetics of stress relaxation are faster than creep and dominated by a decaying exponential

with time constant $\tau_{\text{sr}} = \frac{1}{4} \tau_{\text{creep}}$. These findings are consistent

with the differing kinetics between creep and stress relaxation observed in the demonstration apparatus, and they provide some validation for estimates of its poroelastic properties based upon its structure.

Observations with the demonstration apparatus indicated that stress relaxation reached equilibrium over a characteristic time of approximately 10 seconds (Figure 3), while expansive creep took approximately 10 times longer (Figure 4). In light of the above solutions to Eq. (5), two reasons for this are evident. First, the kinetics of stress relaxation are four times faster. Second, the measurements were made at different thicknesses since stress relaxation occurred at a compressed thickness and expansive creep tended to free-swelling equilibrium. Since the “strain diffusion” exponential time constants scale with the square of thickness [Eq. (12)], this also contributed to the slower kinetics of creep. For assessment of the accuracy of estimates of poroelastic properties (above), insertion of the above estimates for H_A and k under free-swelling conditions into Eqs. (6) and (12) provides $\tau_{\text{creep}} \approx 56$ s, which is reasonably consistent with observations (Figure 4). Discrepancies between this estimate and the observed behavior are most

likely due to errors in the estimation of hydraulic permeability [Eqs. (8) and (9)] and the fact that expansive creep involved non-negligible departures from the free-swelling state so that D_M [Eq. (6)] was not necessarily constant throughout. Nevertheless, the reasonably close correspondence between estimates and observations provides support for estimations of poroelastic properties based upon the demonstration apparatus structure.

Convective dispersion during a single load-release cycle

– The sequence of compressive creep, stress relaxation, and expansive creep outlined above (Figures 2-4) can be repeated with the addition of some dark food coloring to the water above the column in order to illustrate convective dispersion in deforming poroelastic materials. With the demonstration apparatus in the free-swelling state, a few drops of food coloring are added to the fluid above the uppermost block and mixed (without disturbing the column itself) in order to obtain a representation of an elevated concentration of solute above the poroelastic material (Figure 5a). Several minutes can pass without significant change, since transport of the food coloring more deeply into the column occurs by diffusion alone and is a relatively slow process. With compression, fluid is expelled from the column, diluting the coloring in the space above (Figure 5b). During stress relaxation (Figure 5c-d), the boundary conditions of zero fluid flow are respected with the visible result that colored fluid does not enter the column. Then with expansive creep (Figure 5e-f), colored fluid is drawn rapidly into the column and visibly dispersed through its upper region. This dispersion of color through the column provides a clear visual demonstration of the important effects of fluid flows in enhancing solute transport in poroelastic materials, above the transport rates achieved by diffusion alone. Subsequent compression-release cycles result in ever deeper penetration of colored fluid into the column, illustrating the dramatic effects that oscillatory compression can have on enhanced solute transport in poroelastic materials (for example, representing transport of nutrients, growth factors, or other solutes through compressed articular cartilage^(19,20)).

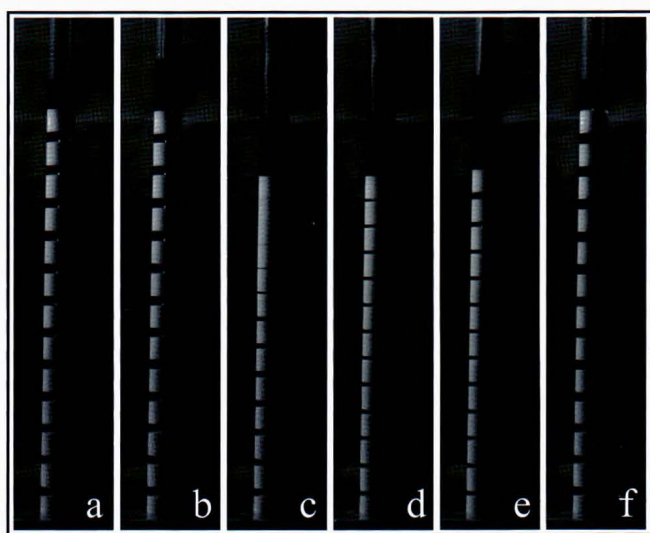


Figure 5. Demonstration of convective dispersion of a small solute in a dynamically compressed poroelastic medium. a) A few drops of food coloring mixed into the fluid space above the column in its free-swelling state do not rapidly penetrate into the column by diffusion alone. b) With the initiation of compressive creep, fluid is expelled from the column, diluting the coloring in the overlying fluid space. From the c) beginning to the d) end of stress relaxation, fluid motion within the column does not affect transport of the coloring in the overlying fluid. e) With the initiation of expansive creep, colored fluid is drawn into the column from above and becomes visible in the spaces between polystyrene blocks. f) Convective dispersion of coloring throughout the upper two-thirds of the column (in the spaces between polystyrene blocks) is evident upon its return to the free-swelling state.

STUDENT REACTIONS

This demonstration apparatus is a valuable teaching tool for helping students visualize the structural changes associated with creep, stress relaxation, and other phenomena associated with poroelastic mechanics. Informal surveys conducted following demonstrations have indicated that the physical (as opposed to computer simulation) nature of the apparatus make it particularly powerful in capturing students’ attention and imaginations. Furthermore, the demonstration appears to remain vivid in students’ memories as more complex phenomena are discussed in lectures that follow. A formal survey of student reactions to the demonstration apparatus (“demo”) was also conducted in accordance with the requirements of the McGill University policy on the ethical conduct

TABLE 1 Student responses to survey questions regarding the effectiveness of the demonstration apparatus. Numerical responses were requested under the following schema: 1 – totally agree; 2 – agree; 3 – neutral; 4 – disagree; 5 – strongly disagree.	
Survey Question	Response (Mean \pm SD; n=11)
The poroelastic mechanics demo was helpful to my ability to visualize what goes on during creep and stress relaxation in poroelastic materials.	1.1 \pm 0.3
After seeing the poroelastic mechanics demo I felt that I had a better ability to appreciate the equations and mathematical problems involved in poroelastic mechanical theory.	1.6 \pm 0.8

TABLE 2 Student comments (edited) when asked “Please provide comments or suggestions for improvement regarding the use of the demo as a teaching aid.”
I found the demo to be very helpful in the interpretation of the equations and the visualization of the concepts.
I really liked your physical demo ... it helped that you were able to ... refer back to it whenever you were explaining a concept or answering a question...
The demo was REALLY helpful! :)
The demo was really helpful in understanding what is happening inside [poroelastic materials] during stress relaxation and creep. ... when students [must] imagine what's going on in ... experiments, their understanding depends on their imagination... The demo helped me to imagine what's happening inside the tissue...
The demo was very helpful. It was very interesting, and I was able to understand what was going on in a fraction of the time it would have taken me if I were to read text about it. I would have never understood to the extent that I do now that I have seen the demonstration...
...among the best demos I've witnessed ...it was simple in design yet it could explain/depict a complex ...phenomenon. ...a hands-on demo is more interesting than one done electronically. A lot of times, we ... learn concepts [from] computer simulations but seldom in real life; it helps a lot to see ... things happen in front of us.
...the demo was definitely really helpful in understanding what is going on ... which in the end helps set up the different problems properly.
The demo really helped me understand what went on during stress relaxation. It was a great visual aid, and I always referred back to it when studying or doing the assignments.
I had a picture in mind already but it's always good to see a real model.
I found it very useful ... because it provides a visual which makes the concepts of stress relaxation and creep much easier to understand.
The demo ... provides [a] way to visualize strain, as a series of spring-loaded sponges in fluid (so to speak), thus creating a simple, thinkable model of a [poroelastic material].

of research involving human subjects. Twenty students in a course in which the apparatus was used to present poroelastic theory were asked to complete the survey; 11 responded. Their quantitative assessment of the helpfulness of the demonstration apparatus for their learning was very positive (Table 1). In addition, their subjective comments (Table 2) provided insights into the (apparently) student-specific ways that the demonstration apparatus can play a role in improving enthusiasm, understanding, and intuition associated with the study of poroelastic mechanics.

INSTRUCTOR EXPERIENCES

The time required for a fairly complete demonstration using the apparatus, including compressive creep, stress relaxation, and expansive creep, is about two minutes (Figures 2-4). This duration is useful in a lecture context: the physical phenomena occur at a rate that is slow enough to follow easily, but a full compression-release cycle can be repeated several times in order to emphasize different aspects of the mechanics involved (*e.g.*, fluid pressurization, fluid flow, consolidation, diffusion of strain) without requiring extended waiting periods.

The apparatus can also be modified straightforwardly in order to alter its kinetics. Such manipulations would provide a basis for using the apparatus even more extensively as an interactive lecture experiment (ILE), which has been proposed as a way to further engage student learning through analysis of demonstrations.^[21] In this context, students could be asked to relate apparatus structure to function. For example, as suggested by Eqs. (8)-(11), changes in block radius a could be used to manipulate the effective hydraulic permeability, while a different choice for the spring constant k_s could be used to manipulate H_A in order to alter the rates of creep and stress relaxation [Eq. (12)]. Effects of material thickness on poroelastic kinetics could also be examined using a different number of block-spring units, without requiring any new component parts.

It is also worth noting that behavior of the apparatus is governed by the diffusion equation [Eq. (5)], and therefore it can also be used to help visualize transport phenomena of more general interest to chemical engineering students. Of particular interest is the stress relaxation transient (Figure 3) since it involves diffusive transport within a region of space of constant thickness. Although the underlying physics is completely different, solute diffusion and conductive heat transfer are also described by the diffusion equation, with solute concentration or material temperature, respectively, appearing in place of the strain (ϵ) in Eq. (5) (and with appropriate modifications to the origins of the diffusion coefficient). Therefore if the “density” of polystyrene blocks is interpreted to represent solute concentration, then the stress relaxation transient (Figure 3) can be considered a representation of the evolution of the solute concentration distribution within a region of fixed thickness, with boundary conditions of zero

solute flux [see discussion of boundary conditions around Eq. (12)]. Similarly, if the “density” of polystyrene blocks is interpreted to represent temperature, then stress relaxation can be considered a representation of the evolution of the temperature distribution within a region of fixed thickness, with boundary conditions of zero heat flux.

CONCLUSIONS

This demonstration apparatus is an effective tool for helping students visualize poroelastic mechanical phenomena, and to spark their interest in discovering structure-function relationships in soft tissues, gels, and other materials. It is particularly helpful because it stimulates attention, discussion, and imagination relating to poroelasticity at an introductory stage. This provides students with a memorable physical demonstration of complex phenomena before they confront the theory. This demonstration strengthens their grasp of the dominant physics before any equations are presented, then provides a reference point to return to once they begin to master the theory and their insights become quantitative.

ACKNOWLEDGMENTS

Supported by the Canada Research Chair program. Contributions from Ananda Tay (apparatus design), Luciano Cusmich (apparatus design and construction), and Derek Rosenzweig (student survey design) are also gratefully acknowledged.

APPENDIX – DETAILS OF CONSTRUCTION

Polystyrene blocks – Individual blocks were machined from a cylindrical bar of polystyrene (McMaster-Carr Part No. 8560K321). Blocks consisted of circular cylinders of length 50 mm and nominal diameter 50 mm (Figure 1a; measured diameter 49.7 mm), with an axially centered protuberance (outer diameter 7.1 mm) on one face and a recess (inner diameter 14.3 mm) on the other (Figure 1b). The protuberance height and recess depth were both 5 mm so that blocks could easily be stacked on one another provided that they were all oriented similarly (*e.g.*, with the protuberance facing up). Protuberance and recess diameters were determined empirically using the constraint that they should interface snugly with conical compression springs (details below) between the blocks.

Transparent column – A clear acrylic (Plexiglas) tube (McMaster-Carr Part No. 8486K515) with inner diameter 50.8 mm and outer diameter 63.5 mm was cut to 110 cm length and mounted in an acrylic base (McMaster-Carr Part No. 8560K321) of geometry 30.5 cm × 30.5 × 2.5 cm (Figure 1c). For mounting, a snug 63.5 mm diameter recession was milled 1.5 cm deep into the center of the base so that one end of the tube could be inserted perpendicularly. The tube was “welded” to the base by treatment of both contacting surfaces with dichloromethane.

Springs – Conical compression springs were selected because of their good force-deformation linearity over large amplitude compression. Springs with unstretched length 31.8 mm, small inner diameter 7.3 mm, large outer diameter 15.2 mm, and spring constant 0.28 N/mm (McMaster-Carr Part No. 1692K36) were chosen.

Assembly – Approximately 250 mL of tap water (viscosity 0.001 Pa·s) was poured into the empty column prior to insertion of polystyrene blocks. With the column tilted to about 30° from horizontal, polystyrene blocks were then introduced to the column, one by one, with their protuberances facing up and already fixed to the small end of a conical spring. As each block was introduced, its bottom surface could therefore be attached to the large end of the conical spring attached to the preceding block. A total of 13 blocks were introduced (and 12 springs). With all blocks introduced, the water volume was then increased to approximately 580 mL, which was sufficient to cover all polystyrene blocks with the structure in a free-swelling state, but not so much as to cause spillage when compression was applied.

Accessories – Compression was applied to the structure manually using a metal rod or the handle of a hammer inserted down the axis of the tube. Very large amplitude compression (to achieve near maximal removal of water from between polystyrene blocks) with the rod was useful for expulsion of air bubbles from the structure just after assembly. During demonstrations, a 4 lb. sledgehammer with handle length 36 cm was used to apply a near-constant force to the structure (to illustrate creep) or to maintain a fixed amount of overall compression of the structure (to illustrate stress relaxation). To demonstrate convective dispersion of small solutes in dynamically compressed poroelastic media, food coloring was used.

Maintenance – When not in use, the demonstration apparatus was drained of water, disassembled, and stored dry to avoid growth of algae or microbes.

REFERENCES

1. Biot, M.A., “General theory of three-dimensional consolidation,” *J. Appl. Phys.*, **12**, 155-164 (1941)
2. Grimshaw, P.E., J.H. Nussbaum, A.J. Grodzinsky, and M.L. Yarmush, “Kinetics of Electrically and Chemically Induced Swelling in Polyelectrolyte Gels,” *J. Chem. Phys.*, **93**, 4462-4472 (1990)
3. Tanaka, T., and D.J. Fillmore, “Kinetics of Swelling of Gels,” *J. Chem. Phys.*, **70**, 1214-1218 (1979)
4. Berkenblit, S.I., T.M. Quinn, and A.J. Grodzinsky, “Molecular Electromechanics of Cartilaginous Tissues and Polyelectrolyte Gels,” *J. Electrostat.*, **34**, 307-330 (1995)
5. Mow, V.C., S.C. Kuei, W.M. Lai, and C.G. Armstrong, “Biphasic Creep and Stress-Relaxation of Articular-Cartilage in Compression—Theory and Experiments,” *J. Biomech. Eng.-T. Asme.*, **102**, 73-84 (1980)
6. King, M.S., “75th Anniversary—Rock-physics developments in seismic exploration: A personal 50-year perspective,” *Geophysics*, **70**, 3nd-8nd (2005)
7. Lee, D.S., and D. Elsworth, “Indentation of a free-failing sharp penetrometer into a poroelastic seabed,” *J. Eng. Mech.-ASCE*, **130**,

- 170-179 (2004)
8. Wysocki, M., L.E. Asp, S. Toll, and R. Larsson, "Two-phase continuum modeling of composites consolidation," *Plast. Rubber Compos.*, **38**, 93-97 (2009)
 9. Fernandez-Barbero, A., I.J. Suarez, B. Sierra-Martin, A. Fernandez-Nieves, F.J. de las Nieves, M. Marquez, J. Rubio-Retama, and E. Lopez-Cabarcos, "Gels and microgels for nanotechnological applications," *Adv. Colloid Interfac.*, **147-48**, 88-108 (2009)
 10. Raemdonck, K., J. Demeester, and S. De Smedt, "Advanced nanogel engineering for drug delivery," *Soft Matter*, **5**, 707-715 (2009)
 11. Han, L., E.H. Frank, J.J. Greene, H.Y. Lee, H.H.K. Hung, A.J. Grodzinsky, and C. Ortiz, "Time-Dependent Nanomechanics of Cartilage," *Biophys. J.*, **100**, 1846-1854 (2011)
 12. Tanaka, Y., A. Kubota, M. Matsusaki, T. Duncan, Y. Hatakeyama, K. Fukuyama, A.J. Quantock, M. Yamato, M. Akashi, and K. Nishida, "Anisotropic Mechanical Properties of Collagen Hydrogels Induced by Uniaxial-Flow for Ocular Applications," *J. Biomat. Sci.-Polym. E.*, **22**, 1427-1442 (2011)
 13. Chin, H.C., G. Khayat, and T.M. Quinn, "Improved characterization of cartilage mechanical properties using a combination of stress relaxation and creep," *J. Biomech.*, **44**, 198-201 (2011)
 14. Abidin, H.Z., H. Andreas, I. Gumilar, Y. Fukuda, Y.E. Pohan, and T. Deguchi, "Land subsidence of Jakarta (Indonesia) and its relation with urban development," *Nat. Hazards*, **59**, 1753-1771 (2011)
 15. Roberts, N., D. Hogg, G.H. Whitehouse, and P. Dangerfield, "Quantitative analysis of diurnal variation in volume and water content of lumbar intervertebral discs," *Clin. Anat.*, **11**, 1-8 (1998)
 16. Thornton, R.K., and D.R. Sokoloff, "Assessing student learning of Newton's laws: The Force and Motion Conceptual Evaluation and the Evaluation of Active Learning Laboratory and Lecture Curricula," *American J. Physics*, **66**, 338-352 (1998)
 17. Sharma, M.D., I.D. Johnston, H. Johnston, K. Varvell, G. Robertson, A. Hopkins, C. Stewart, I. Cooper, and R. Thornton, "Use of interactive lecture demonstrations: A 10-year study," *Physical Review Special Topics - Physics Education Research*, **6**, 1-9 (2010)
 18. Happel, J., "Viscous Flow Relative to Arrays of Cylinders.," *AIChE J.*, **5**, 174-177 (1959)
 19. Evans, R.C., and T.M. Quinn, "Solute convection in dynamically compressed cartilage," *J. Biomech.*, **39**, 1048-1055 (2006)
 20. Zhang, L.H., "Solute Transport in Cyclic Deformed Heterogeneous Articular Cartilage," *Int. J. Appl. Mech.*, **3**, 507-524 (2011)
 21. Moll, R.F., and M. Milner-Bolotin, "The effect of interactive lecture experiments on student academic achievement and attitudes toward physics," *Canadian J. Physics*, **87**, 917-924 (2009) □